HHS Public Access

Author manuscript

Chem Res Toxicol. Author manuscript; available in PMC 2016 October 19.

Published in final edited form as:

Chem Res Toxicol. 2015 October 19; 28(10): 2045–2058. doi:10.1021/acs.chemrestox.5b00256.

Metabolism of an Alkylated Polycyclic Aromatic Hydrocarbon 5-Methylchrysene in Human Hepatoma (HepG2) Cells

Meng Huang[†], **Li Zhang**[†], **Clementina Mesaros**[‡], **Linda C. Hackfeld**[§], **Richard P. Hodge**[§], **Ian A. Blair**[†,‡], and **Trevor M. Penning**[*,†,‡]

[†]Center of Excellence in Environmental Toxicology, University of Pennsylvania, Philadelphia, Pennsylvania 19104-6160, United States

[‡]Center for Cancer Pharmacology, Department of Systems Pharmacology and Translational Therapeutics, Perelman School of Medicine, University of Pennsylvania, Philadelphia, Pennsylvania 19104-6160, United States

[§]Synthetic Organic Chemistry Core, Center in Environmental Toxicology, University of Texas Medical Branch at Galveston, Galveston, Texas 77555-1110, United States

Abstract

Exposure to polycyclic aromatic hydrocarbons (PAHs) in the food chain is the major human health hazard associated with the Deepwater Horizon oil spill. C1-chrysenes are representative PAHs present in the crude oil and have been detected in contaminated sea food in amounts that exceed their permissible safety thresholds. We describe the metabolism of the most carcinogenic C1-chrysene regioisomer, 5-methylchrysene (5-MC), in human HepG2 cells. The structures of the metabolites were identified by HPLC-UV-fluorescence detection and LC-MS/MS. 5-MC-tetraol, a signature metabolite of the diol-epoxide pathway, was identified as reported previously. Novel O-monosulfonated-5-MC-catechol isomers and O-monomethyl-O-monosulfonated-5-MC-catechol were discovered, and evidence for their precursor ortho-quinones was obtained. The identities of O-monosulfonated-5-MC-1,2-catechol, O-monomethyl-O-monosulfonated-5-MC-1,2-catechol, and 5-MC-1,2-dione were validated by comparison to authentic synthesized standards. Dual metabolic activation of 5-MC involving the formation of bis-electrophiles, i.e., a mono-diol-epoxide and a mono-ortho-quinone within the same structure, bis-diol-epoxides, and bis-ortho-quinones is reported for the first time. Evidence was also obtained for minor metabolic conversion of 5-MC to form monohydroxylated-quinones and bis-phenols. The identification of 5-MC-tetraol, O-monosulfonated-5-MC-1,2-catechol, O-monomethyl-O-monosulfonated-5-MC-1,2-catechol,

[*]Corresponding Author Telephone: (215) 898-9445. Fax: (215) 573-0200. penning@upenn.edu.

Supporting Information

The Supporting Information is available free of charge on the ACS Publications website at DOI: 10.1021/acs.chemres-tox.5b00256. Excitation wavelength and emission wavelength spectra of 5-MC (Figure S1); UV spectra of metabolite 1–10 in HepG2 cells (Figure S2); extracted ion chromatograms of Orbitrap full scan for monodehydrated 5-MC-tetraol, bis-dehydrated 5-MC-tetraol, and 5-MC-tetraol detected in HepG2 cells (Figure S3); extracted ion chromatograms of Orbitrap full scan for monodehydrated tetrahydroxy-5-MC-dione (Figure S4); bis-dehydrated-tetraol plus O-monosulfonated-bis-dehydrated-tetraol (Figure S5); monodehydrated-tetraol plus O-mono-glucuronosyl-bis-dehydrated-tetraol (Figure S6); and O-monomethyl-catechol-5-MC-ortho-quinone (Figure S7) detected in HepG2 cells; synthetic routes and details of synthesis of 5-hydroxy-5-MC and 7-hydroxy-5-MC (also see Figure S8) (PDF).

Notes

The authors declare no competing financial interest.

and 5-MC-1,2-dione supports metabolic activation of 5-MC by P450 and AKR isozymes followed by metabolic detoxification of the ortho-quinone through interception of redox cycling by COMT and SULT isozymes. The major metabolites, O-monosulfonated-catechols and tetraols, could be used as biomarkers of human exposure to 5-MC resulting from oil spills.

Abstract

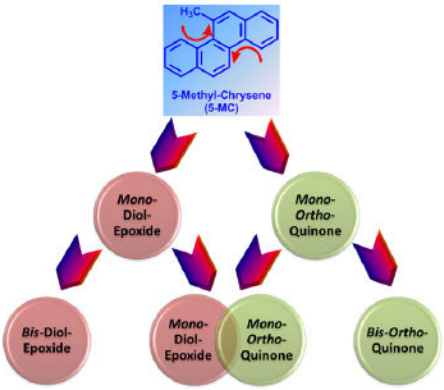

INTRODUCTION

The Deepwater Horizon oil spill in the Gulf of Mexico in 2010 was the largest release of crude oil in U.S. history.[1,2] Polycyclic aromatic hydrocarbons (PAHs) are among the most toxic and persistent components of crude oil.[3] Compositional analysis of the crude oil released identified C1-chrysenes (methyl-chrysenes) as an abundant group of petrogenic PAHs.[4] Contamination of the food chain with petrogenic PAHs is a great concern related to human health.[5] A recent study demonstrated that the concentrations of C1-chrysenes measured from contaminated sea food were 3800-fold higher than the permissible threshold for human consumption recommended by U.S. Environmental Protection Agency (EPA).[6] Among the six regioisomers of C1-chrysenes, 5-methylchrysene (5-MC) was recognized as the most potent carcinogen and tumor initiator in mice.[7]

The toxicity of 5-MC has been associated with metabolic activation mainly via a traditional diol-epoxide pathway in rat and mouse liver S9 fractions, rat liver microsomes, and mouse epidermis as well as in human liver and lung microsomes.[8-12] In this pathway, 5-MC is activated by P450 1A1 to yield the major proximate carcinogen, 5-MC-1*R*,2*R*-diol, which is further converted to the major ultimate carcinogen, 5-MC-1*R*,2*S*-diol-3*S*,4*R*-epoxide.[8-12] This diol-epoxide forms stable N^2-2′-deoxyguanosine (dGuo) adducts *in vitro* and *in vivo*,[13-18] which leads to G to T transversions and other mutations.[19] Another pathway of metabolic activation for 5-MC in mouse skin, whereby hydroxylation on the methyl group catalyzed by P450 3A4 to produce 5-hydroxy-5-MC followed by formation of the activated sulfate ester leads to deoxyadenosine DNA adducts, was proposed.[20-22] However, the formation of 5-hydroxy-5-MC was minimal in most human liver microsomes and was not detected in human lung microsomes.[11]

Human liver is the major target organ for exposure to 5-MC following ingestion. Nevertheless, the metabolism of 5-MC in a human liver cell-based system has not been reported so far. The goal of the present study was to explore the metabolism of 5-MC in human hepatoma (HepG2) cells as a model for primary human hepatocytes.

It was found that the metabolism of 5-MC involved the formation of a diol-epoxide and the formation of an ortho-quinone, and we detected the formation of bis-electrophiles for the first time. Bis-electrophiles involved the formation of a diol-epoxide and an ortho-quinone on different terminal rings within the same structure, the formation of bis-diol-epoxides, and the formation of bis-ortho-quinones. Minor pathways included the formation of a monohydroxylated quinone and the formation of a bis-phenol. We conclude that the diol-epoxide pathway, the ortho-quinone pathway, and their combination likely lead to the metabolic activation of 5-MC following ingestion. O-Monosulfonated-5-MC-catechol conjugates and tetraols were the major metabolites and thus represent human exposure biomarkers for 5-MC and alkylated-PAHs in general that may result from consuming sea food contaminated by crude oil spills.

MATERIALS AND METHODS

Caution: *All PAHs are potentially hazardous and should be handled in accordance with the National Institutes of Health Guidelines for the Laboratory Use of Chemical Carcinogens.*

Chemicals and Reagents

Cell culture media and reagents were purchased from Invitrogen Co. (Carlsbad, CA). Fetal bovine serum (FBS) was purchased from Hyclone (Logan, UT). Human recombinant uridine 5′-diphospho-glucuronosyltransferases (UGT) 2B7 Supersomes (microsomes from baculovirus-infected insect cells expressing UGTs) were purchased from BD Biosciences (San Jose, CA). Human recombinant sulfotransferases (SULT) 1A1 and human recombinant catechol-O-methyltransferase (COMT) were expressed and purified as described by us.[23,24] 5-MC, dithiothreitol, uridine-5′-diphosphoglucuronic acid (UDPGA), adenosine 3′-phosphate 5′-phosphosulfate (PAPS), and *S*-(5′-adenosyl)-L-methionine (AdoMet) chloride were purchased from Sigma-Aldrich Co. (St. Louis, MO). 5-MC-1,2-dione was purchased from MRIGlobal Chemical Carcinogen Repository (Kansas City, MO). 5-Hydroxy-5-MC and 7-hydroxy-5-MC were synthesized as described in the Supporting Information. All solvents were HPLC grade, and all other chemicals used were of the highest grade available.

Enzymatic Synthesis of 5-MC-1,2-Catechol Conjugates

Synthetic routes to four 5-MC-1,2-catechol conjugates are shown in Scheme 1. Experiments were conducted anaerobically in a glovebox purged with argon as described so that 5-MC-1,2-dione could be reduced with dithiothreitol to the catechol.[23-25] We chose human recombinant UGT2B7 and SULT1A1 as the conjugating enzymes because they were the preferred isoforms to form conjugates with benzo[*a*]pyrene-7,8-catechol in our previous studies.[24,25] The reaction conditions for monoglucuronidation, monosulfonation, monomethylation, and bis-conjugation (i.e., monomethylation followed by monosulfonation) of 5-MC-1,2-catechol were the same as described previously,[26] except

that the substrate was replaced by 5-MC-1,2-dione. The negative controls of the four conjugations were prepared without the addition of the respective cofactors. The reaction mixtures were quenched and extracted as described previously[26] and subsequently analyzed by HPLC-UV-Fluorescence (FLR) detection and LC-MS/MS as described below.

Cell Culture

HepG2 (human hepatocellular carcinoma) cells were obtained from American Type Culture Collection and maintained in minimum essential medium (MEM) with 10% heat-inactivated FBS, 2 mM L-glutamine, 100 units/mL penicillin, and 100 μg/mL streptomycin. Cells were incubated at 37 °C in a humidified atmosphere containing 5% CO_2 and were passaged every week at a dilution of 1:7. Cultured cells with a passage number of 10–20 were used in the experiments to reduce variability due to long-term culture conditions. Cultured cells were authenticated by short-terminal repeat DNA analysis and were mycoplasma-free (DNA Diagnostics Center Medical, Fairfield, OH).

Detection and Identification of 5-MC Metabolites in HepG2 Cells

Confluent HepG2 cells were plated in a 6-well plate (~5×10^6). The cells were washed twice and then treated with MEM (without phenol red) containing 10 mM glucose and 1 μM 5-MC (DMSO, 0.2% v/v). The culture media were collected at 0 and 24 h and subsequently acidified with 0.1% formic acid (v/v) before extraction twice with a 1.5-fold volume of cold H_2O-saturated ethyl acetate. The combined organic phases were dried under vacuum, and the residue was reconstituted in methanol (150 μL) and subjected to the following analysis. The resultant aqueous phases were not processed further.

For HPLC-UV-FLR analysis, an aliquot (10 μL) of the reconstituted solution was injected on a tandem Waters Alliance 2695 chromatographic system with a Waters 2996 photodiode array (PDA) detector and a Waters 2475 multi λ FLR detector (Waters Corporation, Milford, MA). Chromatographic separation was achieved on a Zorbax-ODS C18 analytical column (5 μm, 4.6 mm × 250 mm) with a Zorbax-ODS analytical guard column (5 μm, 4.6 mm × 12.5 mm) (DuPont Co., Wilmington, DE) at a room temperature. Mobile phase A was H_2O with 5 mM ammonium acetate and 0.1% trifluoroacetic acid (TFA) (v/v), and mobile phase B was acetonitrile with 5 mM ammonium acetate and 0.1% TFA (v/v). The flow rate was set at 0.5 mL/min. Analytes were eluted with a linear gradient from 5% B to 95% B (v/v) in 30 min, followed by an isocratic hold at 95% B (v/v) for 10 min. At 40 min, B was returned to 5% (v/v) in 1 min and the column was equilibrated for 19 min before the next injection. The total run time for each analysis was 60 min. Eluants from the column were introduced sequentially into the PDA detector and the FLR detector. Excitation (λ_{ex}) and emission (λ_{em}) wavelengths for the FLR detector were set at 273 and 391 nm, respectively, based on the spectral properties of 5-MC.

For ion trap LC-MS/MS analysis, an aliquot (10 μL) of the reconstituted solution was injected on a Waters Alliance 2690 HPLC system (Waters Corporation, Milford, MA) interfaced with a Finnigan LTQ linear ion trap mass spectrometer (Thermo Fisher Scientific, San Jose, CA). The column, mobile phase, flow rate, and linear gradient elution were the same as described above. To prevent extraneous material from entering the mass

spectrometer, the first 10 min of the column eluant was diverted to waste. After that time, the eluants were monitored by the mass spectrometer operated in both positive and negative ion modes with an electrospray ionization (ESI) source. The combination of product ion scan (MS^2), MS/MS/MS (MS^3), and pseudo selected reaction monitoring (SRM) were utilized to analyze the eluants. The mass spectrometry parameters, including spray voltage (3 kV in positive ion mode; 5 kV in negative ion mode), sheath gas flow rate (40 arbitrary units in both ion modes), auxiliary gas flow rate (15 arbitrary units in both ion modes), capillary temperature (275 °C in both ion modes), capillary voltage (38 V in positive ion mode; −19 V in negative ion mode), and tube lens (20 V in positive ion mode; −22.05 V in negative ion mode), were automatically optimized with a 5-MC standard solution in methanol. An isolation width of three bracketed around the *m/z* of interest, activation Q of 0.25, and activation time of 30 ms were used for data acquisition. Xcalibur software, version 2.0 (Thermo Fisher Scientific, San Jose, CA), was used to control the ion-trap LC-MS/MS system and to process data.

In some instances, another aliquot (5 μL) of the reconstituted solution was injected on a nano-Acquity ultra-performance liquid chromatography (UPLC) system (Waters Corporation, Milford, MA) equipped with a LTQ Orbitrap XL mass spectrometer (Thermo Fisher Scientific, San Jose, CA). Chromatographic separation was achieved on a nano-UPLC C18 column (1.7 μm BEH130, 150 μm × 100 mm) (Waters Corporation, Milford, MA) at 50 °C. Mobile phase A was H_2O with 0.1% formic acid (v/v), and mobile phase B was acetonitrile with 0.1% formic acid (v/v). The flow rate was set at 1.6 μL/min. Following an isocratic hold at 5% B (v/v) for 5 min, a linear gradient of 5% to 95% B (v/v) was run over 30 min, followed by an isocratic hold at 95% B (v/v) for another 10 min. At 46 min, B was returned to 5% (v/v) in 2 min and the column was equilibrated for 12 min before the next injection. The total run time for each analysis was 60 min. The mass spectrometer was operated in positive and negative ion modes with a nano-electrospray ionization (nano-ESI) source after accurate calibration with the manufacturer's calibration mixture. The ionization voltage was set to 1.5 kV, and the capillary temperature was set to 200 °C. Full scan spectra were acquired with a resolving power of 60 000 full width at half-maximum in a mass range from *m/z* 100 to 800. Xcalibur software, version 2.0 (Thermo Fisher Scientific, San Jose, CA), was used to control the Orbitrap mass spectrometer and to process data.

RESULTS

Rationale

The metabolism of 1 μM 5-MC in HepG2 cells was selected for the following reasons. One micromolar 5-MC is a reasonable concentration based on estimates of levels of C1-chrsyenes that may be consumed in contaminated sea food.[6] In addition, 1 μM 5-MC was chosen since this is much lower than the reported K_m values for P450 1A1 and 1B1, which have been implicated in its metabolic activation, to ensure that these enzymes are not saturated.[27] We also chose HepG2 cells over human hepatocytes since the latter are limited due to scarce availability, shorter life span, phenotypic instability, and higher individual variability. The metabolites of 5-MC in human HepG2 cells were detected and identified by HPLC-UV-FLR and ion-trap LC-MS/MS. The relative quantitation of the 5-MC metabolites

of interest were obtained from the peak areas on the UV and FLR chromatograms. Preliminary information on 5-MC metabolite structures was obtained by interpreting the corresponding MS^2 and MS^3 spectra of 5-MC metabolites from ion-trap LC-MS/MS. Subsequently, we validated the identities of 5-MC metabolites through a comparison to authentic standards synthesized either chemically or enzymatically.

The optimal pair of λ_{ex} and λ_{em} of 5-MC (Figure S1) was employed to detect its metabolites based on the assumption that most 5-MC metabolites show fluorescence signals under these wavelengths. In our pilot studies of 5-MC metabolism in human HepG2 cells, it was found that most 5-MC metabolites were observed in the organic phase of the extracted media rather than the organic phase of extracted cell pellets and that the most comprehensive metabolite profile from the extracted media was obtained at 24 h (data not shown). Therefore, human HepG2 cells treated with 5-MC at 24 h were selected to identify metabolites.

Four possible routes for 5-MC metabolism were considered to detect and identify metabolites. First, we predicted the diol-epoxide pathway, involving conversion of 5-MC to trans-dihydrodiols followed by formation of diol-epoxides, which can be hydrolyzed to the corresponding tetraols. Second, we predicted the ortho-quinone pathway, involving conversion of trans-dihydrodiols to catechols followed by either formation of phase II conjugates or their oxidation to ortho-quinones, which could be reduced back to the catechols to establish redox cycling. Third, as 5-MC contains two bay regions within its structure, a combination of these two metabolic pathways was also predicted. Lists of the potential metabolites of 5-MC were used to detect bis-electrophiles containing both a diol-epoxide and an ortho-quinone within the same structure in Table 1, the formation of bis-diol-epoxides in Table 2, and the formation of bis-ortho-quinones in Table 3. Fourth, we also predicted that hydroxylation on either the chrysene ring or 5-methyl group side chain followed by formation of phase II conjugates could be another metabolic pathway. On the basis of these predictions, the metabolites of 5-MC were identified.

Detection of 5-MC Metabolites in HepG2 Cells by HPLC-UV-FLR

Comparison of UV chromatograms at λ_{max} 268 nm of the 0 h (Figure 1A) and 24 h (Figure 1B) chromatographic runs showed that ten metabolites of 5-MC were detected in the organic phase of the ethyl acetate-extracted, acidified media from HepG2 cells. The corresponding UV spectra of these ten metabolites were extracted from the PDA detector and are shown in Figure S2. The peak with a retention time of 40.48 min at 0 h was attributed to 5-MC, but it was almost absent at 24 h, suggesting that 5-MC was rapidly metabolized by HepG2 cells over this time course.

Comparison of FLR chromatograms at λ_{ex} 273 nm and λ_{em} 391 nm of the 0 h (Figure 1C) and 24 h (Figure 1D) chromatographic runs showed that there were nine fluorescence peaks in Figure 1D corresponding to metabolites 2–10 in Figure 1B, thus validating that these peaks were derived from 5-MC. The peak corresponding to metabolite 1 with a retention time of 12.62 min was detected only in the UV chromatogram (Figure 1B) but not in the FLR chromatogram (Figure 1D), suggesting the loss of the 5-MC ring fluorophore.

Identification of 5-MC-Tetraol

Monodehydrated 5-MC-tetraol was detected in the culture media from HepG2 cells following treatment with 1 μM 5-MC for 24 h. One peak with a retention time of 17.39 min was detected by monitoring the MS^2 chromatograms (*m/z* 293) at 0 and 24 h in positive ion mode (Table 4). The corresponding MS^2 spectrum (*m/z* 293) of this metabolite showed the sequential loss of H_2O (18 amu) and CO (28 amu) from the protonated molecular ion (Table 4). Comparison of the retention time of monodehydrated 5-MC-tetraol with metabolite 2 on HPLC-UV-FLR in Figure 1 showed excellent agreement.

A single isomer of a monodehydrated 5-MC-tetraol and a single isomer of a bis-dehydrated 5-MC-tetraol were both detected in HepG2 cells with identical retention times by monitoring the extracted ion chromatograms of the Orbitrap full scan at 0 and 24 h in the positive ion mode (Figure S3). A single isomer of an intact 5-MC-tetraol was detected in HepG2 cells that had the same retention time as these two dehydrated products by monitoring the extracted ion chromatograms of the Orbitrap full scan at 0 and 24 h in negative ion mode (Figure S3). Because 5-MC is asymmetric, there are two possible regioisomeric 5-MC-tetraols: those that come from 5-MC-*trans*-1,2-dihydrodiol and those that come from 5-MC-*trans*-7,8-dihydrodiol. However, on the basis of literature precedent,[8-12] we assume that 5-MC-*trans*-1,2-dihydrodiol is formed to yield the corresponding diol-epoxide and tetraol. The resulting tetraol and its absolute configuration cannot be assigned using mass spectrometry. Identification of tetraol indicated the occurrence of the diol-epoxide pathway for the metabolic activation of 5-MC in HepG2 cells.

Identification of O-Monosulfonated-5-MC-1,2-Catechol

O-Monosulfonated-5-MC-catechol isomers were detected in the culture media from HepG2 cells following treatment with 1 μM 5-MC for 24 h. Five isomer peaks at 18.94, 19.46, 22.52, 22.88, 23.18 min were detected by monitoring the MS^3 chromatograms (*m/z* 353 $\rightarrow$ 273 $\rightarrow$) at 0 h (Figure 2A) and 24 h (Figure 2B) in the negative ion mode. The corresponding MS^2 spectra (*m/z* 353) of these five metabolites showed the characteristic loss of sulfate (80 amu) from the deprotonated molecular ion and a representative MS^2 spectrum of the metabolite with a retention time of 22.88 min is shown in Figure 2C. The MS^3 spectrum (*m/z* 353 $\rightarrow$ 273 $\rightarrow$) of this metabolite showed the subsequent loss of one CO group followed by loss of one CH_3 group and one hydrogen (Figure 2D). Comparing the retention times of O-monosulfonated-5-MC-catechol isomers at 18.94, 22.88, 23.18 min with metabolites 3, 5, and 6 on HPLC-UV-FLR in Figure 1 showed that they were in agreement. The specific position of catechol conjugation could not be assigned using mass spectrometry and thus we enzymatically synthesized the 5-MC-catechol-O-sulfate conjugate standards as follows.

In order to generate the O-monosulfonated-5-MC-1,2-catechol standards, 5-MC-1,2-dione was reduced by dithio-threitol followed by phase II conjugation catalyzed by SULT1A1 in the presence of PAPS. After extraction and solvent evaporation, the reaction generated a light yellow solid. HPLC-UV-FLR analysis showed that 5-MC-1,2-dione was completely consumed in the reaction, and two peaks that were absent in the negative control were

observed that eluted earlier than 5-MC-1,2-dione (retention time, 31.98 min) (Figure 3A,B). The major peak had a retention time and UV spectrum identical to those of metabolite 5 in Figure 1. This synthetic product showed a deprotonated molecule $[M - H]^-$ at *m/z* 353 under Q1 full scan in negative ion mode, corresponding to the molecular weight of a deprotonated O-monosulfonated catechol. The fragmentation pattern of this major synthetic product obtained from the MS^2 and MS^3 spectra (Figure 3D,E) was identical to that of metabolite 5 and confirmed its identity as the deprotonated O-monosulfonated-5-MC-1,2-catechol (*m/z* 353). Because 5-MC-1,2-catechol is asymmetric, there are two possible structures of O-monosulfonated-5-MC-1,2-catechol and the specific position of the sulfate group cannot be assigned without characterization by ^1H NMR. The other four O-monosulfonated-5-MC-catechol isomers could be derived from the reduction of 5-MC-7,8-dione, 9,10-dione, or 3,4-dione. Identification of O-monosulfonated-catechol isomers showed that 5-MC was activated by the ortho-quinone pathway.

Identification of O-Monomethyl-O-Monosulfonated-5-MC-1,2-Catechol

O-Monomethyl-O-monosulfonated-5-MC-catechol was detected in the culture media from HepG2 cells following treatment with 1 μM 5-MC for 24 h. One peak with the retention time of 22.54 min was detected by monitoring the pseudo SRM chromatograms (*m/z* 367 $\rightarrow$ 287) at 0 h (Figure 4A) and 24 h (Figure 4B) in negative ion mode, which showed the loss of sulfate (80 amu) from the deprotonated molecular ion. The MS^3 spectrum (*m/z* 367 $\rightarrow$ 287 $\rightarrow$) of this metabolite showed the loss of CH_3 (Figure 4C). This fragmentation pattern is consistent with that observed for O-monomethyl-O-monosulfonated-phenanthrene-9,10-catechol, which was generated in HepG2 cells following incubation with phenanthrene-9,10-quinone.[26] Comparison of the retention time of O-monomethyl-O-monosulfonated-5-MC-catechol with metabolite 4 on HPLC-UV-FLR in Figure 1 showed a good concordance. The specific position of the O-methyl and O-sulfonated groups on 5-MC-catechols could not be assigned using mass spectrometry and thus we enzymatically synthesized bis-catechol conjugate standards as follows.

In order to generate the O-monomethyl-O-monosulfonated-5-MC-1,2-catechol standard, 5-MC-1,2-dione was reduced by dithiothreitol followed by sequential phase II conjugation with COMT plus AdoMet followed by SULT1A1 plus PAPS. After extraction and solvent evaporation, the reaction generated a light yellow solid. HPLC-UV-FLR analysis showed that 5-MC-1,2-dione was completely consumed in the reaction, and a significant peak was observed that eluted slightly later than 5-MC-1,2-dione at 33.11 min (Figure 5A,B), corresponding to O-monomethyl-5-MC catechol. Another two significant peaks with retention times of 22.54 and 23.40 min that were absent in the negative control were also observed that eluted earlier than 5-MC-1,2-dione (Figure 5A–C). The minor peak had the same retention time and UV spectrum as those of metabolite 4 in Figure 1. This polar synthetic product showed a deprotonated molecule $[M - H]^-$ at *m/z* 367 under Q1 full scan in negative ion mode, corresponding to the molecular weight of a deprotonated O-monomethyl-O-monosulfonated catechol. The fragmentation pattern of this synthetic product obtained from the MS^2 and MS^3 spectra (Figure 5D,E) was essentially identical to that of metabolite 4 and confirmed its identity as the deprotonated O-monomethyl-O-monosulfonated-5-MC-1,2-catechol (*m/z* 367). Because 5-MC-1,2-catechol is asymmetric,

there are two possible structures of O-monomethyl-O-monosulfonated-5-MC-1,2-catechol and the specific positions of the methyl and sulfate groups cannot be assigned without characterization by ^{1}H NMR. Identification of O-monomethyl-O-monosulfonated-1,2-catechol indicated the occurrence of the ortho-quinone pathway of 5-MC and also provided evidence for the formation of the intermediate 5-MC-*trans*-1,2-dihydrodiol.

Identification of 5-MC-1,2-Dione and Monohydroxy-5-MC-Dione

Two peaks with retention times of 23.05 and 31.98 min were detected by comparing the pseudo SRM chromatograms (*m/z* 273 → 245) at 0 h (Figure 6A) and 24 h (Figure 6B) in positive ion mode. The respective MS^2 spectra (*m/z* 273) of these two metabolites showed the characteristic loss of CO (28 amu) from the protonated molecular ion, and a representative MS^2 spectrum of the metabolite with a retention time of 31.98 min is shown in Figure 6C. The MS^3 spectrum (*m/z* 273 → 245 →) of this metabolite showed a characteristic loss of a second CO followed by the loss of CH_3 (Figure 6D). The sequential loss of two CO groups supported the presence of an ortho-quinone. When this metabolite was compared to an authentic standard, it had the same retention time and fragmentation pattern as those of 5-MC-1,2-dione, strongly indicating the presence of the ortho-quinone pathway in 5-MC activation.

One peak with a retention time of 31.38 min was detected by comparing the pseudo SRM chromatograms (*m/z* 289 → 260) at 0 h (Figure 7A) and 24 h (Figure 7B) in the positive ion mode. The corresponding MS^2 spectrum (*m/z* 289) of this metabolite (Figure 7C) showed the characteristic loss of CO (28 amu) plus one hydrogen from the protonated molecular ion. The MS^3 spectrum (*m/z* 289 → 260 →) of this metabolite (Figure 7D) showed either another characteristic loss of CO or the loss of $^{\bullet}$CH═C═O. This fragmentation pattern is consistent with that observed for mono-hydroxy-benzo[*a*]-pyrene-7,8-dione, which was detected in three human lung cells after incubation with benzo[*a*]pyrene-7,8-dione (B[*a*]P-7,8-dione).[28] Comparison of the retention time of mono-hydroxy-5-MC-dione with metabolite 10 on HPLC-UV-FLR in Figure 1 showed a good concordance. Mono-hydroxy-5-MC-dione could be derived from either 5-MC-1,2-dione or a remote quinone, and these alternatives cannot be distinguished based on mass spectrometry.

Evidence for the Formation of Bis-Electrophiles

Evidence for dual metabolic activation of 5-MC to form bis-electrophiles (the combination of the diol-epoxide and ortho-quinone pathways) in HepG2 cells was obtained. Two peaks with retention times of 14.66 and 15.65 min were detected by comparing the extracted ion chromatograms of the Orbitrap full scan at 0 h (Figure 8A) and 24 h (Figure 8B) in negative ion mode. MS spectra of these two metabolites both provided the accurate masses and molecular formula of tetrahydroxy-O-monomethyl-5-MC-catechol with acceptable ppm values (Figure 8C,D). In particular, the unique biotransformation of O-methylation strongly indicated the formation of the catechol, thus confirming the occurrence of ortho-quinone pathway. The specific positions of the hydroxy groups of the tetraol and O-monomethyl-catechol could not be assigned using mass spectrometry. Further evidence for the formation of a bis-electrophile containing a diol-epoxide and an ortho-quinone within the same structure came from the detection of two isomers of monodehydrated tetrahydroxy-5-MC-

dione in HepG2 cells when the extracted ion chromatograms of the Orbitrap full scan at 0 and 24 h in positive ion mode were compared (Figure S4).

Bis-dehydrated-tetraol plus O-monosulfonated-bis-dehydrated-tetraol and monodehydrated-tetraol plus O-monoglucuronosyl-bis-dehydrated-tetraol were also detected in HepG2 cells by comparing the extracted ion chromatograms of the Orbitrap full scan at 0 and 24 h in positive ion mode (Figures S5 and S6), indicating the occurrence of activation on the two terminal benzo rings to give a bis-diol-epoxide.

O-Monomethyl-catechol-5-MC-ortho-quinone was also detected in HepG2 cells by comparing the extracted ion chromatograms of the Orbitrap full scan at 0 and 24 h in positive ion mode (Figure S7), indicating the occurrence of the formation of a bis-ortho-quinone. In particular, the unique biotransformation involving O-methylation strongly indicated the formation of the catechol, thus confirming the occurrence of the ortho-quinone pathway.

Identification of Other 5-MC Metabolites

A single isomer of monodehydrated O-monosulfonated-5-MC-dihydro-diol with a retention time of 22.01 min was detected by comparing the pseudo SRM chromatograms (*m/z* 337 → 257) at 0 h (Figure 9A) and 24 h (Figure 9B) in negative ion mode. The corresponding MS^2 spectrum (*m/z* 337) of this metabolite showed the characteristic loss of sulfate (80 amu) from the deprotonated molecular ion (Figure 9C), and the MS^3 spectrum (*m/z* 337 → 257 →) of this metabolite showed the subsequent loss of one CH_3 group (Figure 9D). The specific position of the O-monosulfonated-dihydrodiol could not be assigned using mass spectrometry.

Two isomers of 5-MC-bis-phenols with retention times of 26.96 and 29.93 min were detected by comparing the MS^2 chromatograms (*m/z* 275) at 0 and 24 h in positive ion mode (Table 4). The corresponding MS^2 spectra (*m/z* 275) of these metabolites showed the sequential loss of H_2O (18 amu) and CO (28 amu) from the protonated molecular ion (Table 4). Comparison of the retention time of 5-MC-bis-phenols with metabolites 8 and 9 on HPLC-UV-FLR in Figure 1 showed good agreement. The specific positions of the bis-phenols could not be assigned using mass spectrometry.

5-Hydroxy-5-MC was synthesized as an authentic standard (Figure S8 and Supporting Information) to determine whether any of the metabolites detected in human HepG2 cells supported hydroxylation on the methyl side chain. No metabolite was detected that had a retention time corresponding to the synthetic standard. Negative data were also obtained with 7-hydroxy-5-MC, ruling out formation of this phenol.

DISCUSSION

We describe a comprehensive account of the metabolism of 5-MC in a human liver cell line, HepG2, as a model for human hepatocytes. 5-MC is the most carcinogenic regioisomer of C1-chrysenes present in crude oil, but information about its cellular metabolism in liver is lacking. 5-MC may enter the food chain after oil spills, and elucidating its metabolism in

liver cells is critical in characterizing its potential human toxicity. 5-MC metabolites were detected and identified in HepG2 cell culture media by HPLC-UV-FLR and LC-MS/MS (Table 4). Metabolite 2 in Figure 1 was identified as a tetraol. Metabolites 3, 5, and 6 in Figure 1 were identified as isomers of a O-monosulfonated-catechol. Metabolite 4 in Figure 1 was identified as a O-monomethyl-O-monosulfonated-catechol. Metabolites 8 and 9 in Figure 1 were identified as isomers of a bis-phenol. Metabolite 10 in Figure 1 was identified as a mono-hydroxy-quinone. Metabolites 1 and 7 in Figure 1 remain unassigned. The peak areas on UV and FLR chromatograms provided an estimate of the relative abundance of the metabolites. The major metabolic pathways for the activation of 5-MC in human HepG2 cells involved formation of diol-epoxides and ortho-quinones (Scheme 2). We also observed monohydroxylation of the quinone, as well as bis-hydroxylation to form a bis-phenol (Scheme 2). For the first time, we report evidence for the bioactivation of 5-MC in both bay regions to form bis-electrophiles containing a mono-diol-epoxide and a mono-ortho-quinone within the same structure, bis-diol-epoxides, and bis-ortho-quinones. While the detection of these metabolites was minor, they are inherently reactive since bis-electrophiles have the potential to form protein and DNA cross-links. It is likely that sequestration of these bis-electrophiles by macromolecules contributes to their under detection. The detection of tetraols derived from diol-epoxides and ortho-quinones supports metabolic activation by cytochrome P450 and aldo-keto reductases (AKRs)[29,30] and suggests the presence of phase I enzymes, whereas the detection of catechol conjugates suggests the presence of phase II enzymes. Thus, HepG2 cells contain a battery of enzymes for 5-MC metabolism.

Metabolic activation of 5-MC via the diol-epoxide pathway has been extensively studied previously *in vitro* and *in vivo*.[8-12] Using human liver microsomes, the major metabolites of 5-MC were positional isomers of trans-dihydrodiols and monophenols.[11] In our initial studies, when human HepG2 cells were treated with 5-MC in HBSS media containing 10 mM glucose, two major metabolites, 5-MC-*trans*-1,2-dihydrodiol and 5-MC-*trans*-7,8-dihydrodiol, were detected, and their identities were further validated by comparison to authentic synthesized standards (data not shown). However, under these conditions, a large amount of 5-MC was left unmetabolized after a 24 h incubation, and similar findings were observed in human liver microsomes.[11] We observed enhanced metabolism in human HepG2 cells when grown in MEM (without phenol red) containing 10 mM glucose, where 5-MC was almost completely consumed after a 24 h incubation, and we chose these conditions to conduct our work. The different metabolic outcomes observed in the two cell culture media likely reflect the higher levels of nutrients in MEM vs HBSS media. This enabled us to detect more metabolites, including those derived from the diol-epoxide and ortho-quinone pathways.

HepG2 cells contain inducible P450 1A1, and this is most likely responsible for the formation of diol-epoxides.[31] Previous transcriptomic profiling also demonstrated that HepG2 cells contain AKR1C1, AK1C2, and AKR1C3 but not AKR1C4, which is liver-specific.[32] Several members of the AKR superfamily, including these, are able to oxidize PAH trans-dihydrodiols to ortho-quinones.[29,30] In addition, AKRs, NAD-(P)H:quinone oxidoreductase 1 (NQO1), and carbonyl reductase (CBR) also catalyze the redox cycling of PAH ortho-quinones.[33] Therefore, we hypothesize that AKRs are responsible not only for

the formation of 5-MC-1,2-dione but also for the redox cycling of this ortho-quinone. AKRs are cytosolic and are present in human HepG2 cells rather than in human liver microsomes, which explains why these metabolites were not detected in previous studies using human liver microsomes to metabolize 5-MC.[11] Metabolism of 5-MC in rat liver S9 fractions led to the formation of two unknown metabolites[8] which could have been derived from the ortho-quinone pathway. Rat liver dihydrodiol dehydrogenase (AKR1C9) has been shown to oxidize both 5-MC-*trans*-1,2-dihydrodiol and 5-MC-*trans*-7,8-dihydrodiol to the corresponding quinones.[34,35]

We now identify O-monosulfonated-5-MC-1,2-catechol, O-monomethyl-O-monosulfonated-5-MC-1,2-catechol, and 5-MC-1,2-dione as metabolites by comparison to their authentic synthesized standards. Identification of these three metabolites unequivocally established the metabolic activation of 5-MC via the ortho-quinone pathway involving AKRs in human HepG2 cells. The electrophilic 5-MC-1,2-dione could undergo 1,4- or 1,6-Michael addition with glutathione, DNA, RNA, or protein to form covalent adducts. 5-MC-1,2-dione can also be enzymatically and nonenzymatically reduced back to the catechol and establish futile redox cycles that result in reactive oxygen species (ROS) amplification until cellular reducing equivalents (e.g., NADPH) are depleted. Reduction of 5-MC-1,2-dione to the catechol followed by the formation of phase II conjugates represents a detoxification pathway for 5-MC-1,2-dione since both its electrophilicity and redox activity are eliminated. In contrast, other metabolites such as mono-hydroxy-5-MC-dione, if derived from the ortho-quinone, would retain their electrophilicity and ability to redox cycle, generating oxidative stress and causing oxidative DNA damage.

A novel feature of our work is evidence for the metabolic activation of 5-MC on both terminal benzo rings so that bis-electrophiles containing a mono-diol-epoxide and a mono-ortho-quinone within the same structure, bis-diol-epoxides, and bis-ortho-quinones are formed. This means that P450 1A1 and AKRs can work separately or together in the bioactivation of 5-MC to form bis-electrophiles. Substrate specificity studies demonstrate that the human AKR1C enzymes prefer to metabolize methylated-PAH trans-dihydrodiols and oxidize the (*R*,*R*)- or (*S*,*S*)- stereoisomers equally well.[30]

We failed to show that once 5-MC-*trans*-1,2-dihydrodiol is formed and oxidized to the catechol that either O-monomethylation and/or O-monoglucuronidation occurs in human HepG2 cells using enzymatically synthesized O-monomethyl-5-MC-1,2-catechol and O-monoglucuronosyl-5-MC-1,2-catechol as authentic standards, We expected to find evidence for the O-methyl catechol since we were able to detect O-monomethyl-O-monosulfonated-5-MC-1,2-catechol. This difference could be explained if either the O-monomethyl catechol is rapidly sulfonated or sulfonation proceeds prior to O-methylation.

Using 5-hydroxy-5-MC as an authentic standard, mono-hydroxylation on the methyl group side chain was not observed in human HepG2 cells, which is consistent with previous findings that hydroxymethylation of 5-MC is not an important metabolic activation pathway in humans.[11] Using an authentic standard of 7-hydroxy-5-MC, evidence for monohydroxylation on the chrysene ring was also not found in human HepG2 cells, probably due to the more extensive formation of bis-phenols detected in this study.

The phase I and phase II isozymes responsible for the novel metabolic pathway of 5-MC in human HepG2 cells remain to be completely identified. Detection of 5-MC-1,2-dione, mono-hydroxy-5-MC-dione, and 5-MC-bis-phenols indicates that catalysis is being mediated by cytochrome P450 and AKR in these cells. Although the AKR enzymes responsible for making 5-MC-1,2-dione are likely to be AKR1C1, AKR1C2, and AKR1C3, the P450 isozymes responsible for the hydroxylation of ortho-quinones and bis-phenol formation remain to be identified. The detection of catechol conjugates indicates that 5-MC-1,2-dione is being intercepted to prevent its redox cycling. As human recombinant SULT1A1 can be used to form O-sulfonated-5-MC-1,2-catechol synthetically and is expressed in human HepG2 cells,[36] it is likely to be involved in this detoxication mechanism. Other SULT isoforms expressed in HepG2 cells have yet to be studied to determine their ability to sulfonate 5-MC-1,2-catechol.

Elucidation of the metabolic pathways of 5-MC in human liver cells can be used to identify exposure biomarkers of 5-MC that could be used for biomonitoring human urine and plasma. This study indicates that the major metabolites, i.e., O-monosulfonated-catechol and tetraols, appear to be stable and could be reasonable biomarkers of 5-MC exposure resulting from the consumption of sea food contaminated by oil spills.

Supplementary Material

Refer to Web version on PubMed Central for supplementary material.

Acknowledgments

Funding

This publication was made possible by Deepwater Horizon Research Consortia grant no. U19 ES020676-04 and P30 ES013508 (T.M.P.) from the National Institute of Environmental Health Sciences (NIEHS), NIH, DHHS. UTMB SOCC funding was also provided in part by grant no. P30 ES006676 (Center for Environmental Toxicology, UTMB) from the National Institute of Environmental Health Sciences (NIEHS). Its contents are solely the responsibility of the authors and do not necessarily represent the official views of the NIEHS or NIH.

References

1. Joye SB, MacDonald IR, Leifer I, Asper V. Magnitude and oxidation potential of hydrocarbon gases released from the BP oil well blowout. Nat Geosci. 2011; 4:160–164.
2. Atlas RM, Hazen TC. Oil biodegradation and bioremediation: a tale of the two worst spills in US history. Environ Sci Technol. 2011; 45:6709–6715. [PubMed: 21699212]
3. Goldstein BD, Osofsky HJ, Lichtveld MY. The Gulf oil spill. N Engl J Med. 2011; 364:1334–1348. [PubMed: 21470011]
4. National Institute of Standards and Technology Certificate of Analysis: Standard Reference Material (SRM) 2779, Gulf of Mexico Crude Oil. National Institue of Standards and Technology; Gaithersburg, MD: 2012. p. 1-7.
5. Ylitalo GM, Krahn MM, Dickhoff WW, Stein JE, Walker CC, Lassitter CL, Garrett ES, Desfosse LL, Mitchell KM, Noble BT, Wilson S, Beck NB, Benner RA, Koufopoulos PN, Dickey RW. Federal seafood safety response to the Deepwater Horizon oil spill. Proc Natl Acad Sci U S A. 2012; 109:20274–20279. [PubMed: 22315401]
6. Sammarco PW, Kolian SR, Warby RAF, Bouldin JL, Subra WA, Porter SA. Distribution and concentrations of petroleum hydrocarbons associated with the BP/Deepwater Horizon Oil Spill, Gulf of Mexico. Mar Pollut Bull. 2013; 73:129–143. [PubMed: 23831318]

7. Hecht SS, Bondinell WE, Hoffmann D. Chrysene and methylchrysenes: presence in tobacco smoke and carcinogenicity. J Natl Cancer Inst. 1974; 53:1121–1133. [PubMed: 4427391]
8. Hecht SS, LaVoie E, Mazzarese R, Amin S, Bedenko V, Hoffmann D. 1,2-dihydro-1,2-dihydroxy-5-methylchrysene, a major activated metabolite of the environmental carcinogen 5-methylchrysene. Cancer Res. 1978; 38:2191–2194. [PubMed: 350385]
9. Melikian AA, LaVoie EJ, Hecht SS, Hoffmann D. 5-Methylchrysene metabolism in mouse epidermis *in vivo*, diol epoxide–DNA adduct persistence, and diol epoxide reactivity with DNA as potential factors influencing the predominance of 5-methylchrysene-1,2-diol-3,4-epoxide–DNA adducts in mouse epidermis. Carcinogenesis. 1983; 4:843–849. [PubMed: 6872139]
10. Amin S, Huie K, Balanikas G, Hecht SS, Pataki J, Harvey RG. High stereoselectivity in mouse skin metabolic activation of methylchrysenes to tumorigenic dihydrodiols. Cancer Res. 1987; 47:3613–3617. [PubMed: 3594428]
11. Koehl W, Amin S, Staretz ME, Ueng YF, Yamazaki H, Tateishi T, Guengerich FP, Hecht SS. Metabolism of 5-methylchrysene and 6-methylchrysene by human hepatic and pulmonary cytochrome P450 enzymes. Cancer Res. 1996; 56:316–324. [PubMed: 8542586]
12. Shappell NW, Carlino-MacDonald U, Amin S, Kumar S, Sikka HC. Comparative metabolism of chrysene and 5-methylchrysene by rat and rainbow trout liver microsomes. Toxicol Sci. 2003; 72:260–266. [PubMed: 12655039]
13. Melikian AA, LaVoie EJ, Hecht SS, Hoffmann D. Influence of bay-region methyl group on formation of 5-methylchrysene dihydrodiol epoxide:DNA adducts in mouse skin. Cancer Res. 1982; 42:1239–1242. [PubMed: 7060000]
14. Melikian AA, Amin S, Hecht SS, Hoffmann D, Pataki J, Harvey RG. Identification of the major adducts formed by reaction of 5-methylchrysene *anti*-dihydrodiol-epoxides with DNA *in vitro*. Cancer Res. 1984; 44:2524–2529. [PubMed: 6547075]
15. Reardon DB, Prakash AS, Hilton BD, Roman JM, Pataki J, Harvey RG, Dipple A. Characterization of 5-methylchrysene-1,2-dihydrodiol-3,4-epoxide-DNA adducts. Carcinogenesis. 1987; 8:1317–1322.
16. Melikian AA, Amin S, Huie K, Hecht SS, Harvey RG. Reactivity with DNA bases and mutagenicity toward Salmonella typhimurium of methylchrysene diol epoxide enantiomers. Cancer Res. 1988; 48:1781–1787. [PubMed: 3258179]
17. Melikian AA, Prahalad KA, Amin S, Hecht SS. Comparative DNA binding of polynuclear aromatic hydrocarbons and their dihydrodiol and bay region diolepoxide metabolites in newborn mouse lung and liver. Carcinogenesis. 1991; 12:1665–1670. [PubMed: 1893526]
18. Kuljukka-Rabb T, Peltonen K, Isotalo S, Mikkonen S, Rantanen L, Savela K. Time- and dose-dependent DNA binding of PAHs derived from diesel particle extracts, benzo[*a*]pyrene and 5-methychrysene in a human mammary carcinoma cell line (MCF-7). Mutagenesis. 2001; 16:353–358. [PubMed: 11420405]
19. Bigger CA, Flickinger DJ, Strandberg J, Pataki J, Harvey RG, Dipple A. Mutational specificity of the *anti* 1,2-dihydrodiol 3,4-epoxide of 5-methylchrysene. Carcinogenesis. 1990; 11:2263–2265. [PubMed: 2176139]
20. Okuda H, Hiratsuka A, Nojima H, Watabe T. A hydroxymethyl sulphate ester as an active metabolite of the carcinogen, 5-hydroxymethylchrysene. Biochem Pharmacol. 1986; 35:535–538. [PubMed: 3456226]
21. Okuda H, Nojima H, Watanabe N, Miwa K, Watabe T. Activation of the carcinogen, 5-hydroxymethylchrysene, to the mutagenic sulphate ester by mouse skin sulphotransferase. Biochem Pharmacol. 1988; 37:970–973. [PubMed: 2964238]
22. Okuda H, Nojima H, Miwa K, Watanabe N, Watabe T. Selective covalent binding of the active sulfate ester of the carcinogen 5-(hydroxymethyl)chrysene to the adenine residue of calf thymus DNA. Chem Res Toxicol. 1989; 2:15–22. [PubMed: 2519226]
23. Zhang L, Jin Y, Chen M, Huang M, Harvey RG, Blair IA, Penning TM. Detoxication of structurally diverse polycyclic aromatic hydrocarbon (PAH) *o*-quinones by human recombinant catechol-*O*-methyltransferase (COMT) via *O*-methylation of PAH catechols. J Biol Chem. 2011; 286:25644–25654. [PubMed: 21622560]

24. Zhang L, Huang M, Blair IA, Penning TM. Detoxication of benzo[*a*]pyrene-7,8-dione by sulfotransferases (SULTs) in human lung cells. J Biol Chem. 2012; 287:29909–29920. [PubMed: 22782890]
25. Zhang L, Huang M, Blair IA, Penning TM. Interception of benzo[*a*]pyrene-7,8-dione by UDP glucuronosyltrans-ferases (UGTs) in human lung cells. Chem Res Toxicol. 2013; 26:1570–1578. [PubMed: 24047243]
26. Huang M, Zhang L, Mesaros C, Zhang S, Blaha MA, Blair IA, Penning TM. Metabolism of a representative oxygenated polycyclic aromatic hydrocarbon (PAH) phenanthrene-9,10-quinone in human hepatoma (HepG2) cells. Chem Res Toxicol. 2014; 27:852–863. [PubMed: 24646012]
27. Shimada T, Oda Y, Gillam EM, Guengerich FP, Inoue K. Metabolic activation of polycyclic aromatic hydrocarbons and other procarcinogens by cytochromes P450 1A1 and P450 1B1 allelic variants and other human cytochromes P450 in Salmonella typhimurium NM2009. Drug Metab Dispos. 2001; 29:1176–1182. [PubMed: 11502724]
28. Huang M, Liu X, Basu SS, Zhang L, Kushman ME, Harvey RG, Blair IA, Penning TM. Metabolism and distribution of benzo[*a*]pyrene-7,8-dione (B[*a*]P-7,8-dione) in human lung cells by liquid chromatography tandem mass spectrometry: detection of an adenine B[*a*]P-7,8-dione adduct. Chem Res Toxicol. 2012; 25:993–1003. [PubMed: 22480306]
29. Palackal NT, Burczynski ME, Harvey RG, Penning TM. The ubiquitous aldehyde reductase (AKR1A1) oxidizes proximate carcinogen *trans*-dihydrodiols to *o*-quinones: potential role in polycyclic aromatic hydrocarbon activation. Biochemistry. 2001; 40:10901–10910. [PubMed: 11535067]
30. Palackal NT, Lee SH, Harvey RG, Blair IA, Penning TM. Activation of polycyclic aromatic hydrocarbon *trans*-dihydrodiol proximate carcinogens by human aldo-keto reductase (AKR1C) enzymes and their functional overexpression in human lung carcinoma (A549) cells. J Biol Chem. 2002; 277:24799–24808. [PubMed: 11978787]
31. Burczynski ME, Penning TM. Genotoxic polycyclic aromatic hydrocarbon ortho-quinones generated by aldo-keto reductases induce CYP1A1 via nuclear transloaction of the aryl hydrocrabon receptor. Cancer Res. 2000; 60:908–915. [PubMed: 10706104]
32. Steckelbroeck S, Oyesanmi B, Jin Y, Lee SH, Kloosterboer HJ, Penning TM. Tibolone metabolism in human liver is catalyzed by 3α/3β-hydroxysteroid dehydrogenase activities of the four isoforms of the aldo-keto reductase (AKR)1C subfamily. J Pharmacol Exp Ther. 2006; 316:1300–1309. [PubMed: 16339391]
33. Shultz CA, Quinn AM, Park JH, Harvey RG, Bolton JL, Maser E, Penning TM. Specificity of human aldo-keto reductases, NAD(P)H:quinone oxidoreductase, and carbonyl reductases to redox-cycle polycyclic aromatic hydrocarbon diones and 4-hydroxyequilenin-*o*-quinone. Chem Res Toxicol. 2011; 24:2153–2166. [PubMed: 21910479]
34. Smithgall TE, Harvey RG, Penning TM. Regio- and stereospecificity of homogeneous 3α-hydroxysteroid-dihydrodiol dehydrogenase for *trans*-dihydrodiol metabolites of polycyclic aromatic hydrocarbons. J Biol Chem. 1986; 261:6184–6191. [PubMed: 3457793]
35. Smithgall TE, Harvey RG, Penning TM. Spectroscopic identification of *ortho*-quinones as the products of polycyclic aromatic *trans*-dihydrodiol oxidation catalyzed by dihy-drodiol dehydrogenase. A potential route of proximate carcinogen metabolism. J Biol Chem. 1988; 263:1814–1820. [PubMed: 3276678]
36. Westerink WM, Schoonen WG. Phase II enzyme levels in HepG2 cells and cryopreserved primary human hepatocytes and their induction in HepG2 cells. Toxicol In Vitro. 2007; 21:1592–1602. [PubMed: 17716855]

ABBREVIATIONS

PAPS	adenosine 3′-phosphate 5′-phosphosulfate
AdoMet	*S*-(5′-adenosyl)-L-methionine
AKR	aldo-keto reductase

B[*a*]P-7,8-dione	benzo[*a*]pyrene-7,8-dione
CBR	carbonyl reductase
COMT	catechol-O-methyltransferase
P450	cytochrome P450
ESI	electrospray ionization
FBS	fetal bovine serum
HPLC-UV-FLR	high-performance liquid chromatography-ultraviolet-fluorescence
LC-MS/MS	liquid chromatography–tandem mass spectrometry
5-MC	5-methylchrysene
NQO1	NAD (P)H:quinone oxidoreductase 1
PAH	polycyclic aromatic hydrocarbon
ROS	reactive oxygen species
SULTs	sulfotransferases
UDPGA	uridine-5′-diphosphoglucuronic acid
UGTs	uridine 5′-diphospho-glucuronosyltransferases

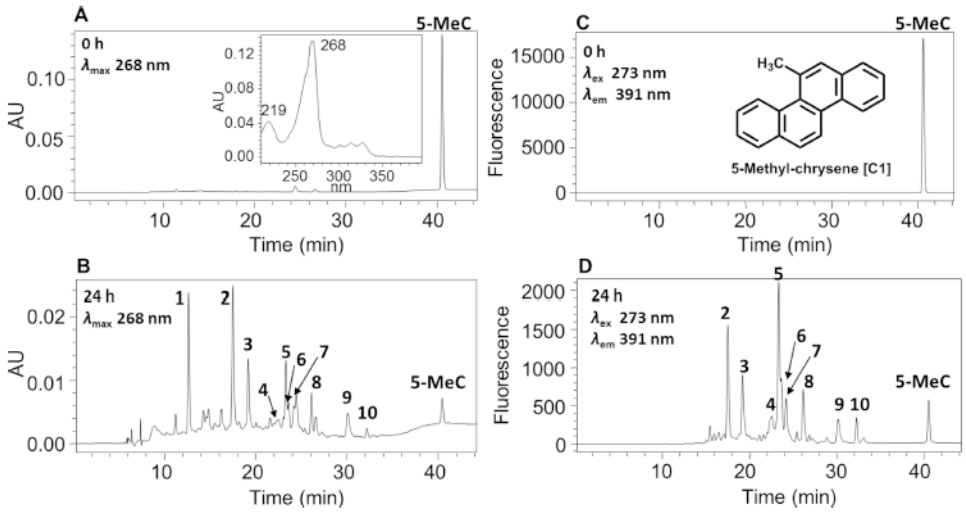

Figure 1.

HPLC detection of 5-MC metabolites in human HepG2 cells. (A) UV chromatogram at λ_{max} 268 nm at 0 h. (B) UV chromatogram at λ_{max} 268 nm at 24 h. (C) FLR chromatogram at λ_{ex} 273 nm and λ_{em} 391 nm at 0 h. (D) FLR chromatogram at λ_{ex} 273 nm and λ_{em} 391 nm at 24 h. Human HepG2 cells (~5×10^6) were treated with 5-MC (1 μM, 0.2% (v/v) DMSO) in MEM (without phenol red) containing 10 mM glucose. The cell media were collected at 0 and 24 h and subsequently acidified with 0.1% formic acid before extraction with ethyl acetate. The extracts were analyzed on a HPLC-UV-FLR. 5-MeC = 5-methylchrysene.

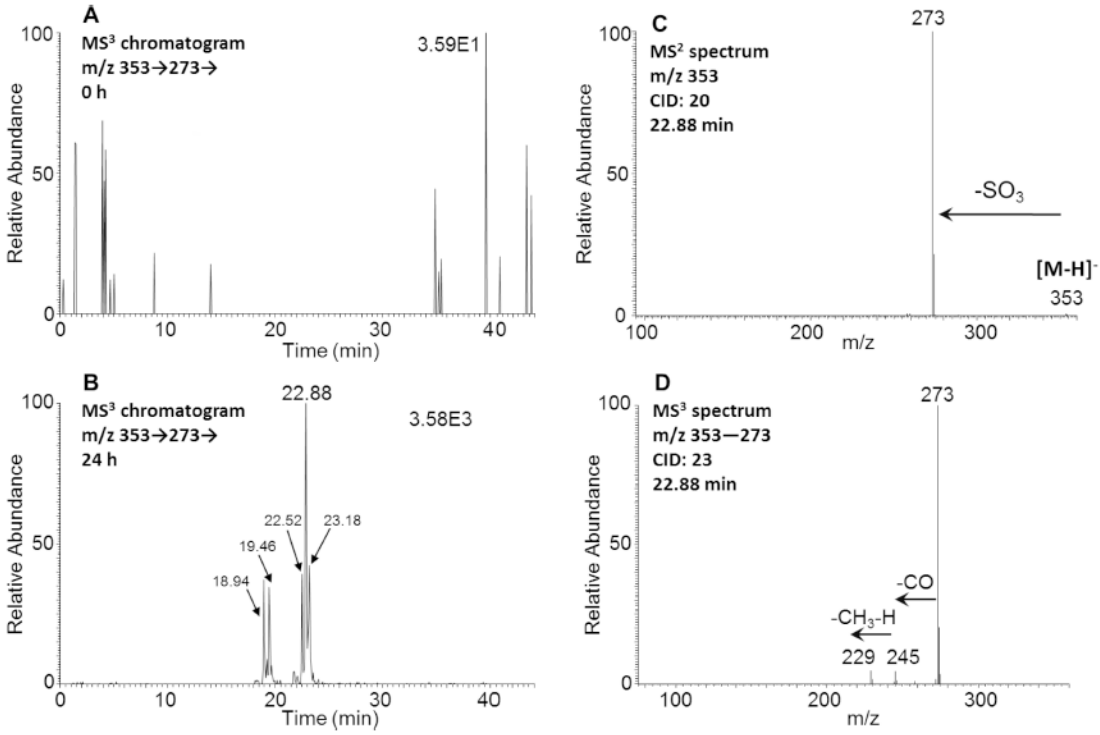

Figure 2.

Detection of O-monosulfonated-5-MC-catechol isomers in human HepG2 cells. (A) MS^3 chromatogram at 0 h. (B) MS^3 chromatogram at 24 h. (C) MS^2 spectrum of the peak at 22.88 min. (D) MS^3 spectrum of the peak at 22.88 min. The samples were prepared as described in the caption to Figure 1 and were subsequently analyzed on an ion-trap LC-MS/MS.

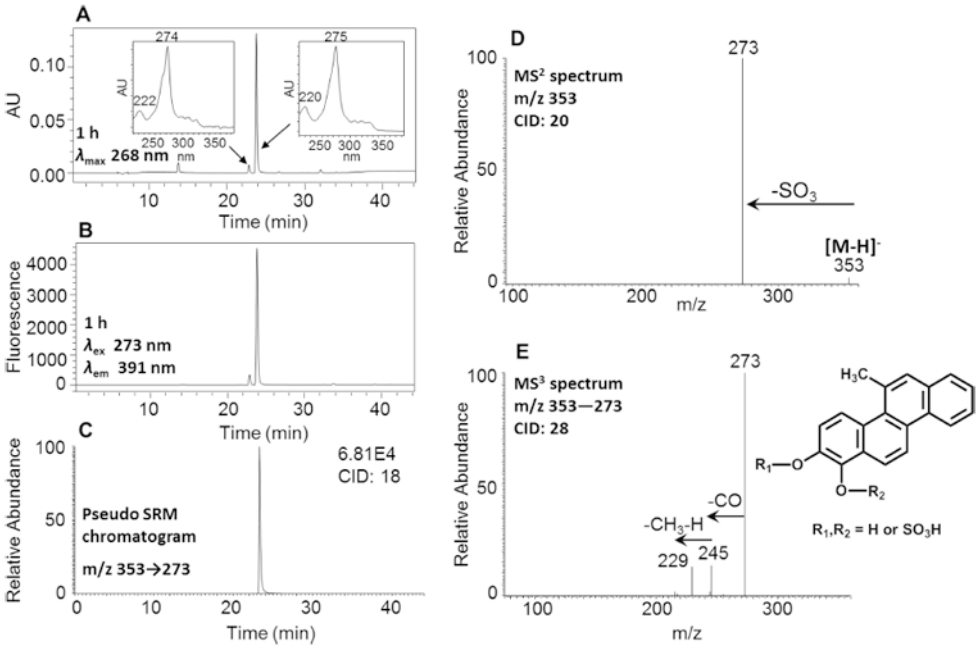

Figure 3.

Characterization of synthetic O-monosulfonated-5-MC-1,2-catechol. (A) UV chromatogram at λ_{max} 268 nm. (B) FLR chromatogram at λ_{ex} 273 nm and λ_{em} 391 nm. (C) Extracted ion chromatogram of pseudo SRM transition. (D) MS^2 spectrum. (E) MS^3 spectrum. The product profiles were obtained after 1 h incubation of 5-MC-1,2-catechol with SULT1A1 and PAPS.

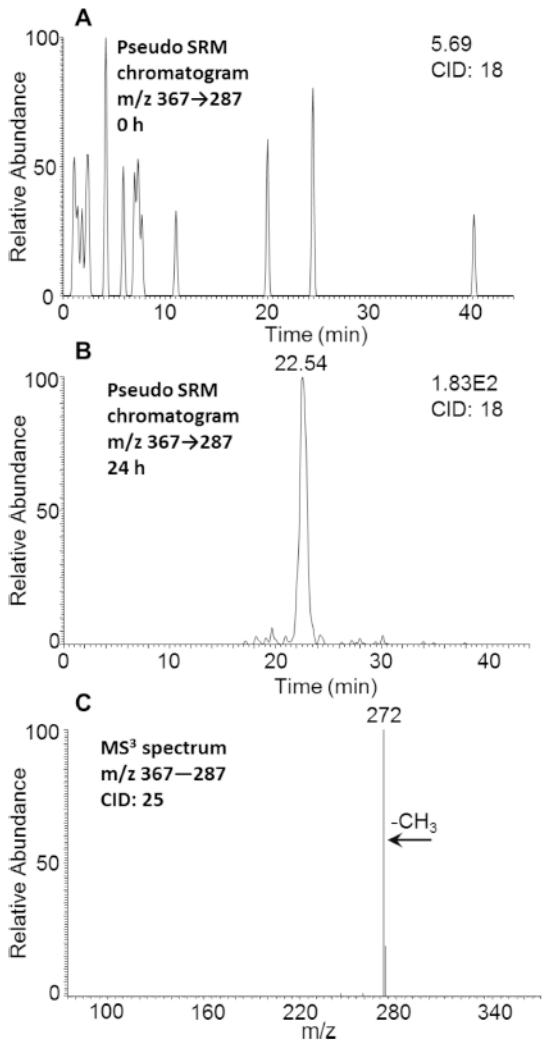

Figure 4.

Detection of O-monomethyl-O-monosulfonated-5-MC-1,2-catechol in human HepG2 cells. (A) Extracted ion chromatogram of pseudo SRM transition at 0 h. (B) Extracted ion chromatogram of pseudo SRM transition at 24 h. (C) MS^3 spectrum of the peak at 22.54 min. The samples were prepared as described in the caption to Figure 1 and were subsequently analyzed on an ion-trap LC-MS/MS.

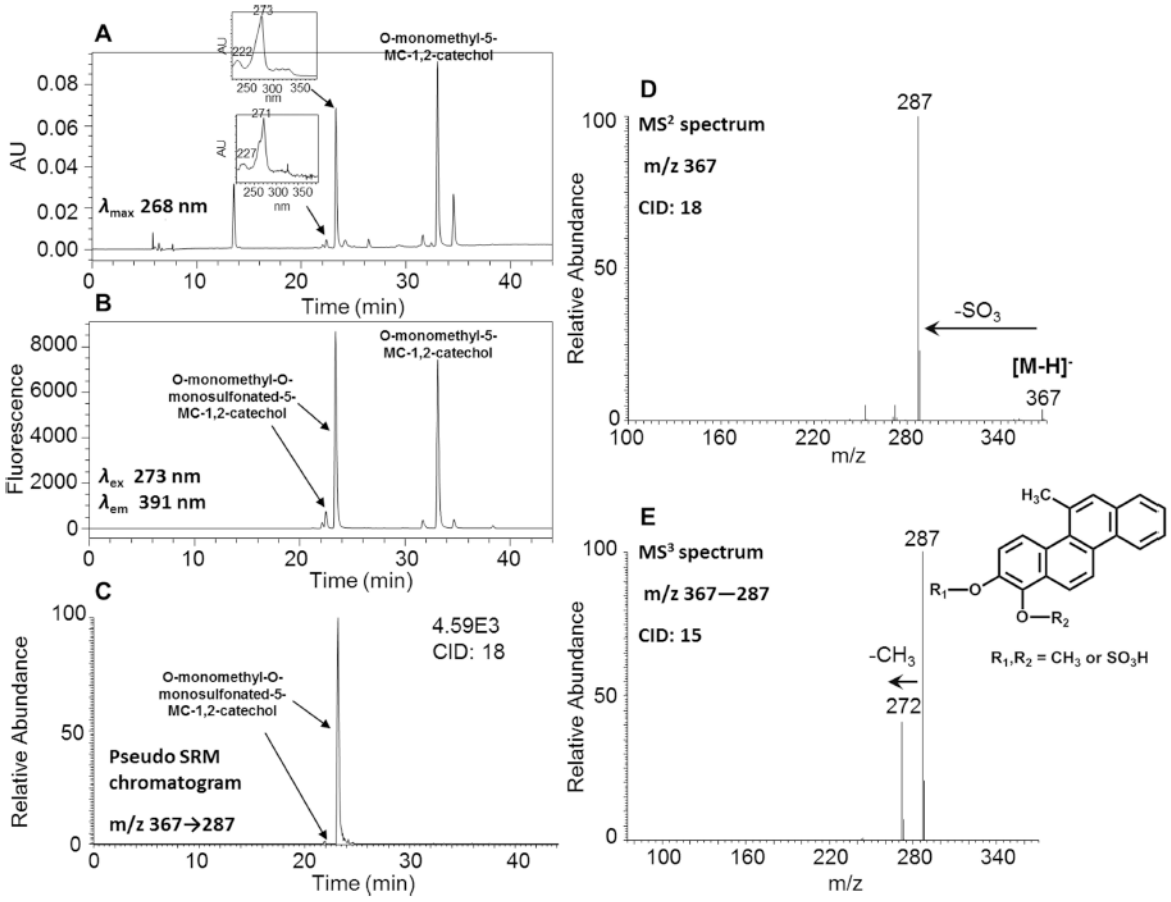

Figure 5.

Characterization of synthetic O-monomethyl-O-monosulfonated-5-MC-1,2-catechol. (A) UV chromatogram at λ_{max} 268 nm. (B) FLR chromatogram at λ_{ex} 273 nm and λ_{em} 391 nm. (C) Extracted ion chromatogram of pseudo SRM transition. (D) MS^2 spectrum. (E) MS^3 spectrum. The product profiles were obtained after 1 h incubation of 5-MC-1,2-catechol with COMT and AdoMet followed by an additional 1 h incubation with SULT1A1 and PAPS.

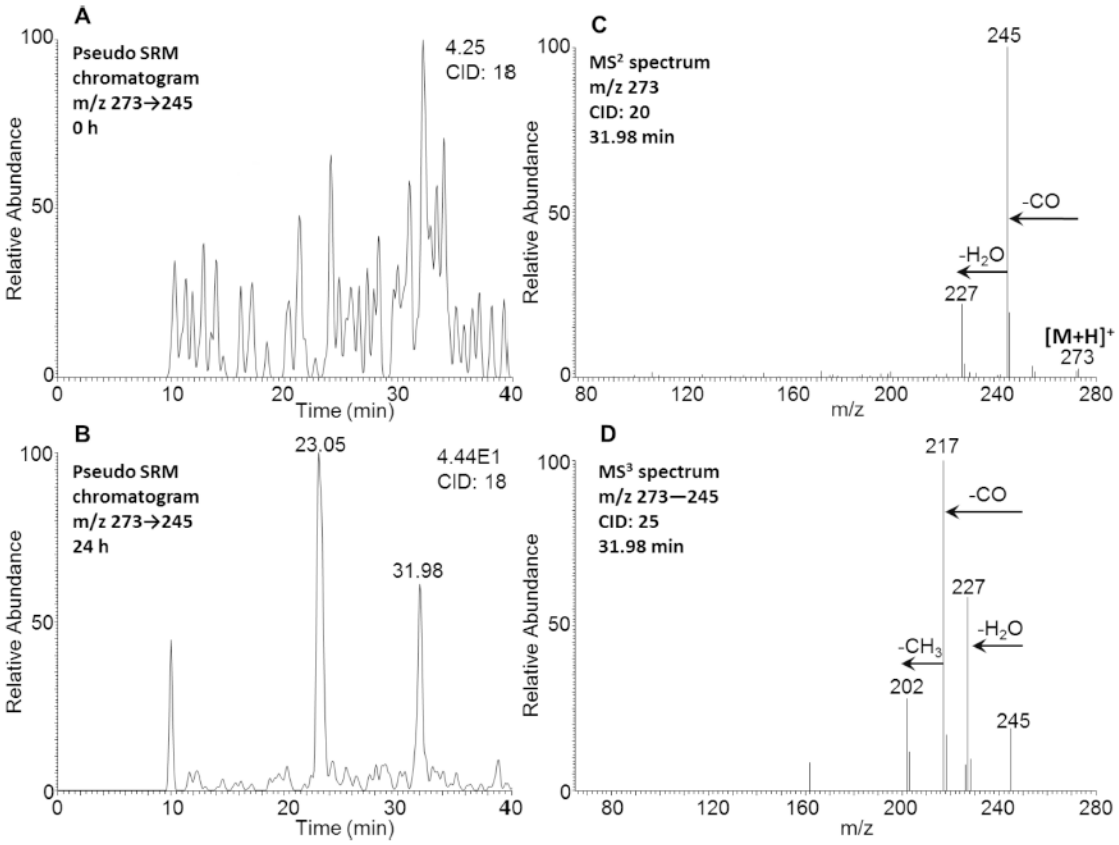

Figure 6.

Detection of 5-MC-1,2-dione in human HepG2 cells. (A) Extracted ion chromatogram of pseudo SRM transition at 0 h. (B) Extracted ion chromatogram of pseudo SRM transition at 24 h. (C) MS^2 spectrum of the peak at 31.98 min. (D) MS^3 spectrum of the peak at 31.98 min. The samples were prepared as described in the caption to Figure 1 and were subsequently analyzed on an ion-trap LC-MS/MS. Another peak with a retention time of 23.05 min and with relatively high polarity could be an isomer of O-monosulfonated-5-MC-catechol, which could undergo cleavage of the sulfate conjugate in the mass spectrometer followed by auto-oxidation and thus result in the detection of quinone instead.

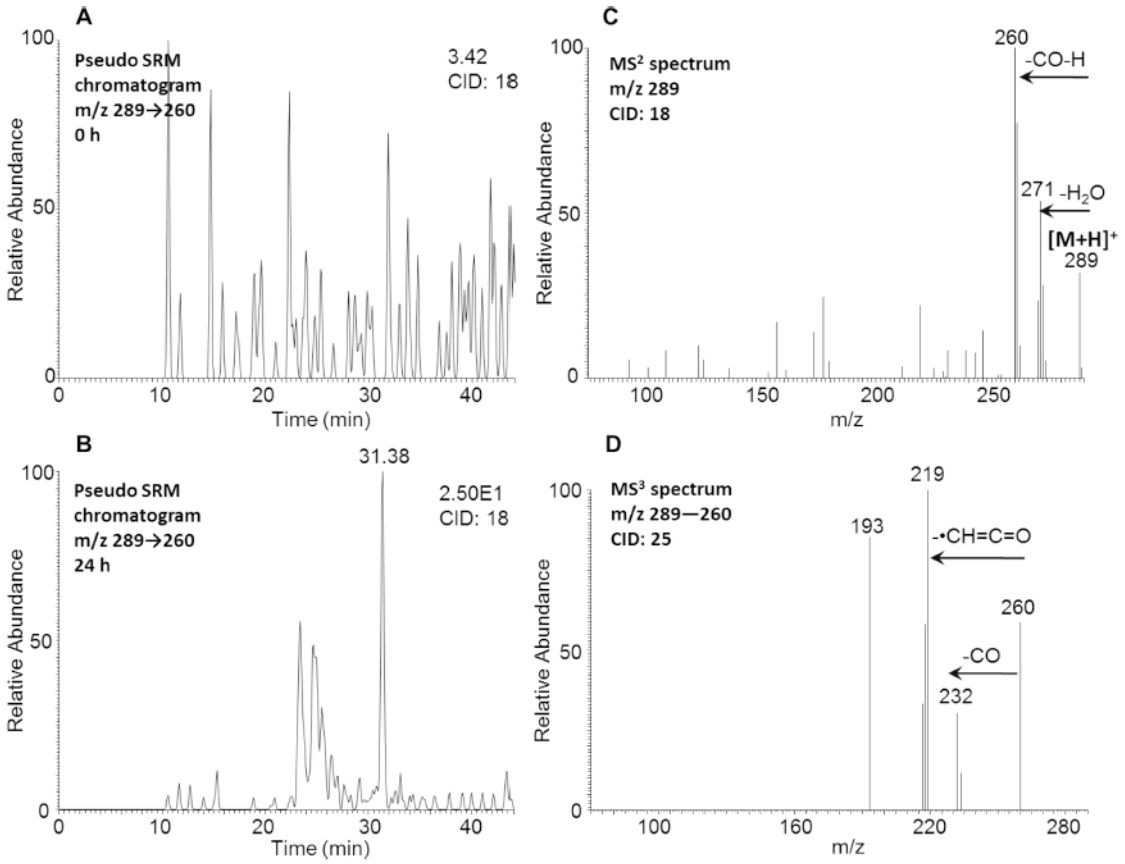

Figure 7.

Detection of mono-hydroxy-5-MC-dione in human HepG2 cells. (A) Extracted ion chromatogram of pseudo SRM transition at 0 h. (B) Extracted ion chromatogram of pseudo SRM transition at 24 h. (C) MS^2 spectrum of the peak at 31.38 min. (D) MS^3 spectrum of the peak at 31.38 min. The samples were prepared as described in the caption to Figure 1 and were subsequently analyzed on an ion-trap LC-MS/MS.

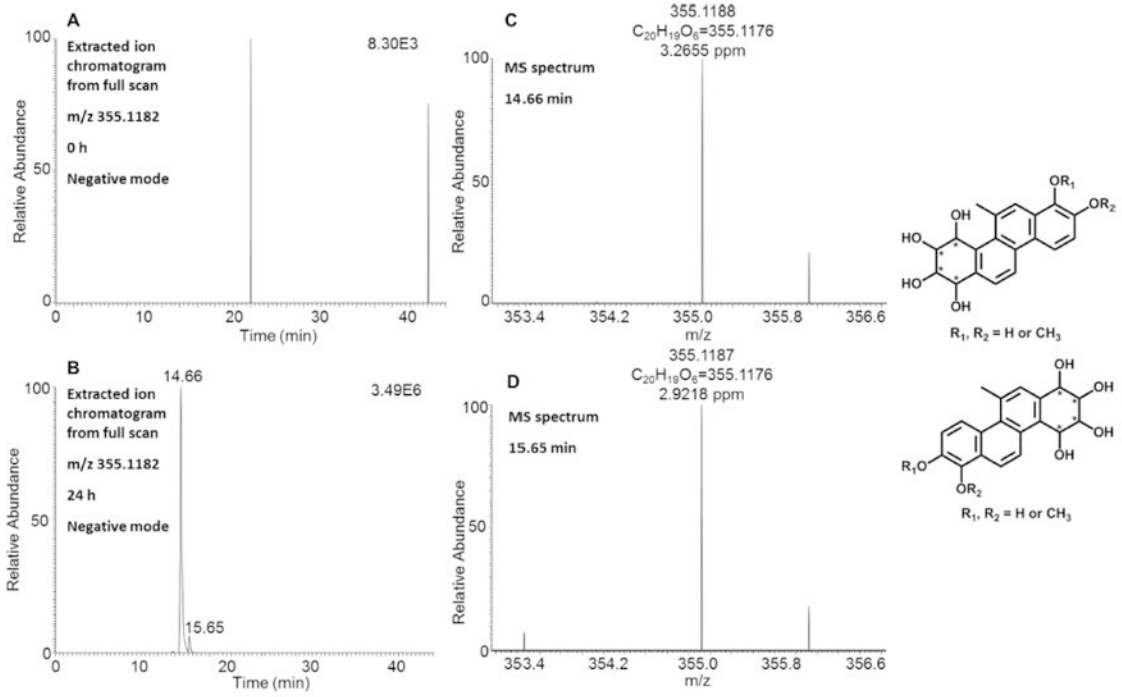

Figure 8.

Detection of tetrahydroxy-O-monomethyl-5-MC-catechols in human HepG2 cells. (A) Extracted ion chromatogram of the Orbitrap full scan at 0 h. (B) Extracted ion chromatogram of the Orbitrap full scan at 24 h. (C, D) MS spectra of the peaks eluting at 14.66 and 15.65 min. The samples were prepared as described in the caption to Figure 1 and were subsequently analyzed on an Orbitrap LC-MS/MS.

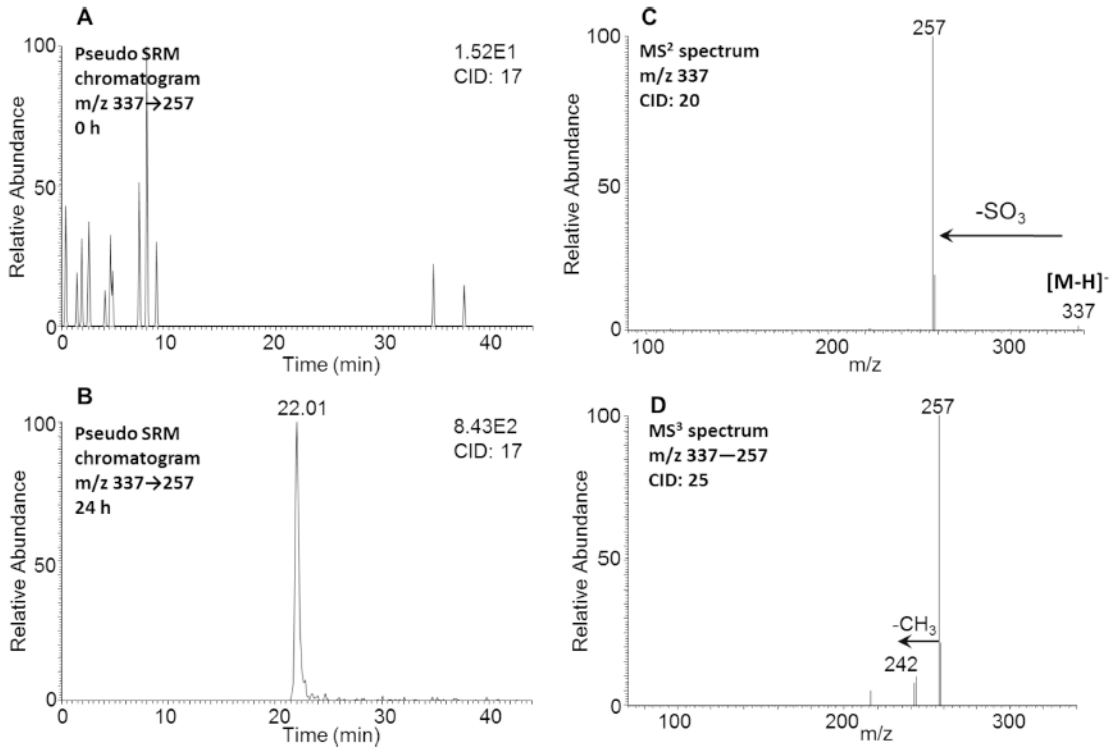

Figure 9.

Detection of monodehydrated O-monosulfonated-5-MC-dihydrodiol in human HepG2 cells. (A) Extracted ion chromatogram of pseudo SRM transition at 0 h. (B) Extracted ion chromatogram of pseudo SRM transition at 24 h. (C) MS^2 spectrum of the peak at 22.01 min. (D) MS^3 spectrum of the peak at 22.01 min. The samples were prepared as described in the caption to Figure 1 and were subsequently analyzed on an ion-trap LC-MS/MS.

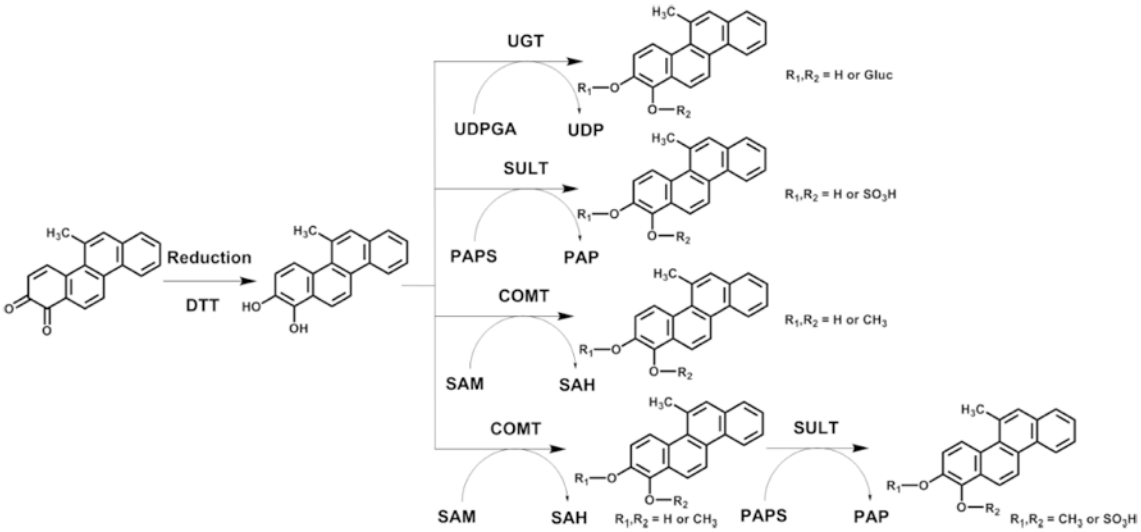

Scheme 1. Synthetic Routes of Four 5-MC-1,2-Catechol Conjugates

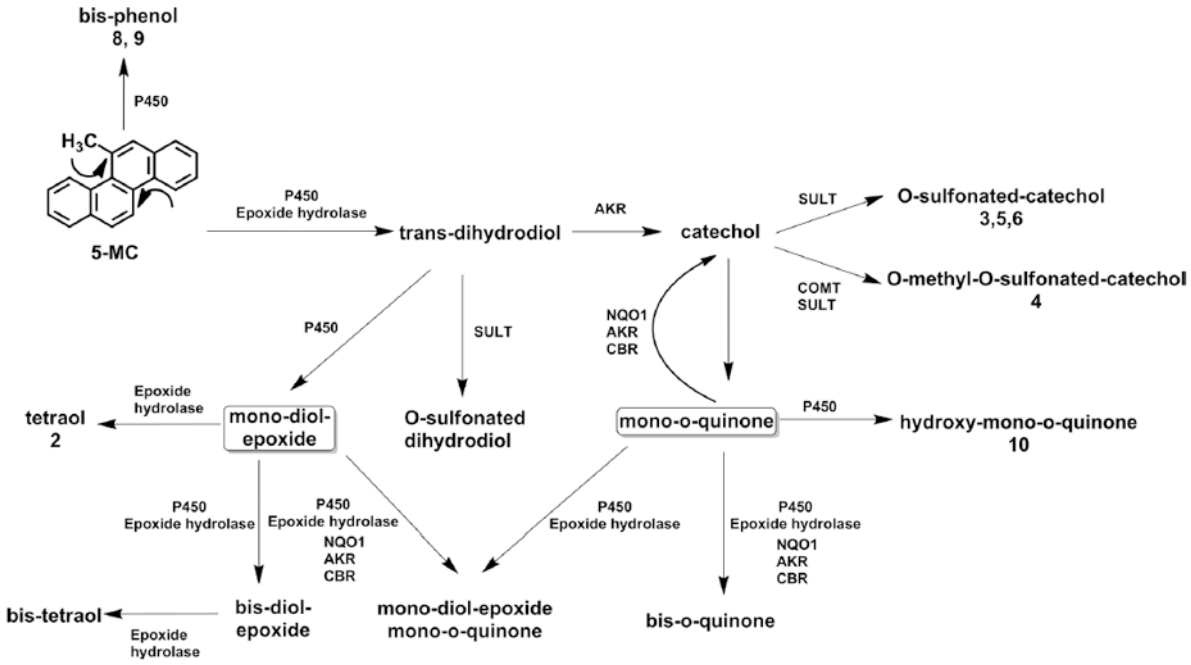

Scheme 2. Proposed Metabolic Pathway of 5-MC in Human HepG2 Cells[a]

[a]The numbers for each metabolite correspond to the metabolites labeled in the UV and fluorescence chromatograms in Figure 1.

Table 1

Accurate Masses of Potential 5-MC Metabolites in HepG2 Cells That Result from the Formation of Bis-Electrophiles Containing both a Diol-Epoxide and an Ortho-Quinone

5-MC metabolites	molecular formula	positive mode	negative mode
Tetraol + O-quinone	$C_{19}H_{16}O_6$	341.1025	339.0869
Monodehydrated tetraol + O-quinone	$C_{19}H_{14}O_5$	323.0919	321.0763
Bis-dehydrated tetraol + O-quinone	$C_{19}H_{12}O_4$	305.0814	303.0657
Tetraol + O-methyl catechol	$C_{20}H_{20}O_6$	357.1338	355.1182
Monodehydrated tetraol + O-methyl catechol	$C_{20}H_{18}O_5$	339.1232	337.1076
Bis-dehydrated tetraol + O-methyl catechol	$C_{20}H_{16}O_4$	321.1127	319.0970
Tetraol + O-sulfonated catechol	$C_{19}H_{18}O_9S$	423.0750	421.0593
Monodehydrated tetraol + O-sulfonated catechol	$C_{19}H_{16}O_8S$	405.0644	403.0488
Bis-dehydrated tetraol + O-sulfonated catechol	$C_{19}H_{14}O_7S$	387.0538	385.0382
Tetraol + O-glucuronosyl catechol	$C_{25}H_{26}O_{12}$	519.1503	517.1346
Monodehydrated tetraol + O-glucuronosyl catechol	$C_{25}H_{24}O_{11}$	501.1397	499.1240
Bis-dehydrated tetraol + O-glucuronosyl catechol	$C_{25}H_{22}O_{10}$	483.1291	481.1135
Tetraol + O-methyl-O-sulfonated catechol	$C_{20}H_{20}O_9S$	437.0906	435.0750
Monodehydrated tetraol + O-methyl-O-sulfonated catechol	$C_{20}H_{18}O_8S$	419.0801	417.0644
Bis-dehydrated tetraol + O-methyl-O-sulfonated catechol	$C_{20}H_{16}O_7S$	401.0695	399.0538

Table 2

Accurate Masses of Potential 5-MC Metabolites in HepG2 Cells That Result from the Formation of Bis-Diol-Epoxides

5-MC metabolites	molecular formula	positive mode	negative mode
Tetraol + Tetraol	$C_{19}H_{22}O_8$	379.1393	377.1236
Monodehydrated tetraol + Tetraol	$C_{19}H_{20}O_7$	361.1287	359.1131
Monodehydrated tetraol + Monodehydrated tetraol (or Bis-dehydrated tetraol + Tetraol)	$C_{19}H_{18}O_6$	343.1182	341.1025
Monodehydrated tetraol + Bis-dehydrated tetraol	$C_{19}H_{16}O_5$	325.1076	323.0919
Bis-dehydrated tetraol + Bis-dehydrated tetraol	$C_{19}H_{14}O_4$	307.0970	305.0814
Tetraol + O-sulfonated tetraol	$C_{19}H_{22}O_{11}S$	459.0961	457.0805
Monodehydrated tetraol + O-sulfonated tetraol	$C_{19}H_{20}O_{10}S$	441.0855	439.0699
Monodehydrated tetraol + Monodehydrated O-sulfonated tetraol (or Bis-dehydrated tetraol + O-sulfonated tetraol)	$C_{19}H_{18}O_9S$	423.0750	421.0593
Monodehydrated tetraol + Bis-dehydrated O-sulfonated tetraol	$C_{19}H_{16}O_8S$	405.0644	403.0488
Bis-dehydrated tetraol + Bis-dehydrated O-sulfonated tetraol	$C_{19}H_{14}O_7S$	387.0538	385.0382
Tetraol + O-glucuronosyl tetraol	$C_{25}H_{30}O_{14}$	555.1714	553.1557
Monodehydrated tetraol + O-glucuronosyl tetraol	$C_{25}H_{28}O_{13}$	537.1608	535.1452
Monodehydrated tetraol + Monodehydrated O-glucuronosyl tetraol (or Bis-dehydrated tetraol + O-glucuronosyl tetraol)	$C_{25}H_{26}O_{12}$	519.1503	517.1346
Monodehydrated tetraol + Bis-dehydrated O-glucuronosyl tetraol	$C_{25}H_{24}O_{11}$	501.1397	499.1240
Bis-dehydrated tetraol + Bis-dehydrated O-glucuronosyl tetraol	$C_{25}H_{22}O_{10}$	483.1291	481.1135

Table 3

Accurate Masses of Potential 5-MC Metabolites in HepG2 Cells That Result from the Formation of Bis-Ortho-Quinones

5-MC metabolites	molecular formula	positive mode	negative mode
O-quinone + O-quinone	$C_{19}H_{10}O_4$	303.0657	301.0501
O-quinone + O-methyl catechol	$C_{20}H_{14}O_4$	319.0970	317.0814
O-quinone + O-sulfonated catechol	$C_{19}H_{12}O_7S$	385.0382	383.0225
O-quinone + O-glucuronosyl catechol	$C_{25}H_{20}O_{10}$	481.1135	479.0978
O-quinone + O-methyl-O-sulfonated catechol	$C_{20}H_{14}O_7S$	399.0538	397.0382
O-methyl catechol + O-methyl catechol	$C_{21}H_{18}O_4$	335.1283	333.1127
O-methyl catechol + O-sulfonated catechol	$C_{20}H_{16}O_7S$	401.0695	399.0538
O-methyl catechol + O-glucuronosyl catechol	$C_{26}H_{24}O_{10}$	497.1448	495.1291
O-sulfonated catechol + O-sulfonated catechol	$C_{19}H_{14}O_{10}S_2$	467.0107	464.9950
O-sulfonated catechol + O-glucuronosyl catechol	$C_{25}H_{22}O_{13}S$	563.0859	561.0703
O-glucuronosyl catechol + O-glucuronosyl catechol	$C_{31}H_{30}O_{16}$	659.1612	657.1456

Table 4

Mass Transitions for 5-Methylchrysene Metabolites in HepG2 Cells

metabolite No.	5-MC metabolites	retention time (min)	mode	*m/z*
2	Monodehydrated tetraol	17.39	positive	293 $[M + H]^+$,
				275 $[M + H - H_2O]^+$,
				247 $[M + H - H_2O - CO]^+$,
				257 $[M + H - 2H_2O]^+$,
				229 $[M + H - 2H_2O - CO]^+$
3, 5, 6	O-sulfonated catechol	18.94, 19.46, 22.52, 22.88, 23.18	negative	353 $[M - H]^-$,
				273 $[M - H - SO_3]^-$,
				245 $[M - H - SO_3 - CO]^-$,
				229 $[M - 2H - SO_3 - CO - CH_3]^-$
4	O-methyl-O-sulfonated catechol	22.54	negative	367 $[M - H]^-$,
				287 $[M - H - SO_3]^-$,
				272 $[M - H - SO_3 - CH_3]^-$
–	Ortho-quinone	31.98	positive	273 $[M + H]^+$,
				245 $[M + H - CO]^+$,
				227 $[M + H - CO - H_2O]^+$,
				217 $[M + H - 2CO]^+$,
				202 $[M + H - 2CO - CH_3]^+$
10	Monohydroxy-quinone	31.38	positive	289 $[M + H]^+$,
				271 $[M + H - H_2O]^+$,
				260 $[M + H - CO - {}^{\bullet}H]^+$,
				232 $[M + H - 2CO - {}^{\bullet}H]^+$,
				219 $[M + H - CO - {}^{\bullet}CH{=}C{=}O - {}^{\bullet}H]^+$
–	Dehydrated O-sulfonated dihydrodiol	22.01	negative	337 $[M - H]^-$,
				257 $[M - H - SO_3]^-$,
				242 $[M - H - SO_3 - CH_3]^-$
8, 9	Bis-phenol	26.96, 29.93	positive	275 $[M + H]^+$,
				257 $[M + H - H_2O]^+$,
				246 $[M + H - CO - {}^{\bullet}H]^+$,
				229 $[M + H - H_2O - CO]^+$